# BIOPHYSICAL INSIGHTS INTO THE AGGREGATION MECHANISM OF OVALBUMIN

**Manjumol Mathew[1], Charuvila T. Aravindakumar[2], Usha K. Aravind[3]***
[1]St. George's College, Aruvithura,[2]School of Environmental Sciences, Mahatma Gandhi University, Kottayam-686 560, India [3]School of Environmental Studies Cochin University of Science and Technology, Kochi-682022, India
*Correspondence to: *E-mail: uka@cusat.ac.in Phone: 0481 2732120.

## Abstract

This work illustrates the possible share of environmental toxins in inducing protein misfolding and hence protein aggregation. This is brought out by the interaction studies of ovalbumin (OVA) with mercuric chloride (denaturant) using time resolved, steady state, atomic force microscopy spectroscopy (AFM). The steady state quenching experiments showed a three state sigmoidal transition pattern indicates a concentration dependent quenching. More insight about the fibrillation pathway at molten globule state is brought out using AFM studies. Various oligomeric structures of OVA are encountered during the study with the addition of different concentrations of $HgCl_2$. Time dependent atomic force microscopy study exposed the formation of fibrils in the end state.

## 1. Introduction

Though the subject had been debated for years, studies on metal ion protein interaction has more relevance in the present scenario. The probabilities of coming across diseases caused by protein polymerization such as Alzheimer, dementia, emphysema, and liver cirrhosis have increased in the modern times (Squitti and Polimanti 2013). There can be a number of reasons which may lead to perturbation of protein structure, eventually leading to polymerization and hence loosening its functions (Gettins 2002, Hatcher, Hong et al. 2008). There are high chances either through dermal or dietary exposure, biomolecules are vulnerable to endocrine disrupting compounds, pharmaceutically active compounds, personal care products and many more toxic matrices (Ibrahim, Ibrahim et al. 2010, Mathew, Sreedhanya et al. 2014). Among this, the interaction with protein has its own relevance being the carrier of exogeneous ligands. Spectroscopic studies are the most popular tool to

study such interactions. The intrinsic fluorescence of some proteins has already been utilized to study the metal ion binding interaction. These include serum albumins and proteins of the serpin family. Some of the most toxic heavy metal ions have been a subject of this interaction studies such as Hg, Cd, Zn, Ni etc (Tamás, Sharma et al. 2014, Tamás, Fauvet et al. 2018, Lopes de Andrade, Marreilha Dos Santos et al. 2021). There have been many reported incidences due to the toxic effect of inorganic Hg that results either from direct or indirect bioaccumulation. Whatever may be the case, Hg is always a hot topic as far as the toxicity is concerned.

In this respect the study on the interaction of Hg with proteins (especially serpin group) are expected to provide vital information regarding conformational transition. These protein misfolding diseases can be initiated by a number of environmental triggers, leading to cellular toxic intermediates (β-sheet oligomers). The oligomeric forms of amyloidogenic proteins interact with cell membranes and are known to perturb structural integrity and permeation character (Bhattacharya and Dogra 2015, Dalal, Arya et al. 2015). The health crisis due to human degenerative diseases have initiated investigations to identify the cellular toxic β-sheet rich intermediates of proteins, their mechanistic pathways that lead to fibrillar formation and the subsequent interaction with cellular membranes. The findings indicate that the low molecular weight soluble oilgomers and the high molecular weight protofibrils are more toxic than the final insoluble fibrils which form the amyloid plaque. The constituents of the plaques are different in different diseases, for instance, Aβ peptide in AD, α-synuclein fibrils, Parkinson's disease (PD), and islet amyloid polypeptide (IAPP) in type II diabetes (Jacobsen, Reinhart et al. 2005, Pan, Wang et al. 2016). The final fibrillar stage and the very early conformational transitions are easier to investigate than the heterogeneous prefibrilar stage. The intermediate stages and oligomerization dynamics is more interesting from the therapeutic point of view.

Formation of toxic intermediate structures is common feature found in protein aggregation pathways. Rather than the final fibrilar stage the steps leading to the formation of intermediates and possible mechanism of their assembly is far more crucial. Herein we report the mechanism of formation of defolded state of ovalbumin, a model serpin at molten globule state (pH 2.2) on exposure to increasing concentration of mercuric chloride (denaturant). We combine different spectroscopic and microscopic techniques to study the intermediate oligomers and protofibrils.

## 2. EXPERIMENTAL SECTION

### 2.1 Materials.

Ovalbumin was purchased from Sigma-Aldrich and was used without further purification. Protein solutions (1 mg/ml) were prepared in buffer. $HgCl_2$ was prepared in water. Ultra-pure water was used for the preparation of all the solutions and buffers. Glycine-HCl (pH 2.5, 3), was used for buffer preparations. Mercuric chloride ($HgCl_2$) from Merck-India was used as received. All other chemicals were of analytical grade and were used as supplied. All other reagents were of analytical grade. The pH of the buffer was checked with digital pH meter (model 335 Systronics, Kochi).

### 2.2 Steady-State Measurements.

The fluorescence measurements were carried out on a LS55 (Perkin Elmer) having a 20 kW continuous powered high pressure Xe-lamp as the excitation source and an R928 photomultiplier as the photodetector. The excitation and emission slits were set at 5 nm. Ovalbumin was excited at 295 nm in order to minimize the contribution from Tyrosine (Tyr). The fluorescence emission was collected from 300 to 600 nm

### 2.2 Time-Resolved Fluorescence Measurements.

Time–resolved fluorescence decay measurements were carried out by time-correlated single photon counting using Horiba Jobin Yvon spectrometer. A pulsed diode ($\lambda_{max}$ = 295 nm) was used as the excitation source and emission was monitored at respective emission wavelengths. The data was analyzed by using DAS6 software attached with the system.

### 2.3 AFM:

Structural characterization of protein aggregate is attempted by using confocal Raman microscopy coupled with an atomic force microscopy (AFM) instrument (Witec ALPHA 300RA, Germany). The AFM measurements have been carried out in the noncontact mode, with silicon tip of 75 kHz resonant frequency and 2.8 N/m force constant (radius below 8nm). Data was then collected using a multimode fiber into a high throughput lens based spectrograph (UHTS 300) with 300 mm focal length and grating 1800 g/mm, blazed at 500 nm. The microscope base is also equipped with an active vibration isolation system, active in the range 0.7−1000 Hz. The acquired spectra and AFM images are processed and analysed using the Witec Project 4 program.

## 3. RESULT AND DISCUSSION

### 3.1 AFM analysis of OVA at molten globule state

The topographical feature of self-assembled nanoscale structures of OVA was recorded using AFM. The structural feature of OVA with the addition of different concentrations of $HgCl_2$ is shown in figure 1. The detailed morphological analysis of OVA at acidic pH has been demonstrated in several reports (Bhattacharya and Mukhopadhyay 2012). In our study we have characterized the structural transformation of OVA at pH 2.2 with the addition of denaturant. Prior to the addition of denaturant "V" shaped monomers were observed (Fig. 1A). The statistical analysis revealed that these oligomers have height of 10-30 nm (Fig. 1C) and width of 178 nm (Fig. 1A). Upon the addition of 1.25 µM HgCl2 bead like oligomers are formed. The protofibrils formed have an average height of 5-20 nm. Compared with the molten globule structure we can observe a gradation in the average height of protofibrils formed. On the other hand the width remained the same. Further addition of 3 µM HgCl2 (Region II), results in the formation of long protofibrils with the height of 5-20 nm (Fig. 1 F) and width decreased to 165 nm (Fig. 1B). The careful monitoring of AFM image revealed the progressive increase in the length elongation of the protofibrils formed. In order to known about the detailed mechanism of protein aggregation, the SV (Stern-Volmer) plot and life time decay plot of OVA are utilised with the help of steady-state fluorescence experiments.

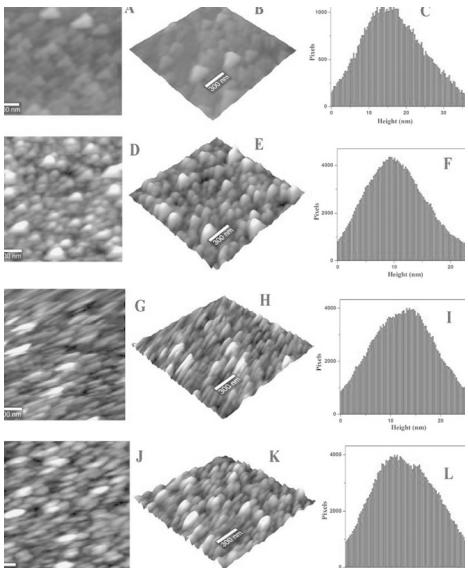


**Figure 1:** AFM images of (A): OVA pH 2.2 before exposure (scale bar is

300 nm throughout) showing "V" shaped monomers; (B): and (C): the corresponding 3D representation and height profile, (D): "bead like oligomers" after exposure to 1.25 μM HgCl2; (E): and (F): the corresponding 3D representation and height profile; (G): Long protofibrils with the increment of HgCl2 to 2.5 μM (H): and (I): the corresponding 3D representation and height profile (J) protofibrils formed by lateral addition with the increment of HgCl2 to 6.25 μM (K): and (L): the corresponding 3D representation and height profile.

### 3.2 Fluorescence spectroscopy

Fluorescence spectroscopy is a reliable tool to study the interaction of pollutants with proteins due to its great sensitivity and capability to probe different microenvironments (Albrecht 2008, Lamba, Paul et al. 2009, Anand, Jash et al. 2010). Any changes in the fluorescence intensity or shift in the emission maximum normally indicate conformational changes in the protein. The intrinsic fluorescence spectra of OVA in the presence of a series of concentrations of $HgCl_2$ are collected at an excitation wavelength of 295 nm. Figure 2A represents the variation of fluorescence intensity of OVA with the different concentration of $HgCl_2$. The figure clearly depicts that with the initial addition of quencher molecule up to 1.5 μM, the florescence intensity reduced only to a small extent. Increasing the concentration of $HgCl_2$ to 2.5 μM results in the further reduction in fluorescence intensity of OVA to a significant level. Further addition of $HgCl_2$ has no influence on the fluorescence intensity of OVA. In order to know the mechanism of quenching of OVA, the binding constant ($K_b$), number of binding site (n) were calculated using the modified version of Stern-Volmer equation.

$$\log\left[\frac{(F_0 - F)}{F}\right] = \log K_b + n \log[Q] \qquad (1)$$

Where $F_0$ and F are the steady-state fluorescence intensities in the absence and in the presence of quencher, respectively, $K_{sv}$ is the Stern-Volmer quenching constant and [Q] is the concentration of quencher (BPS). $\tau_0$ is the average lifetime of the protein without the quencher. $K_b$ reflects the degree of interaction of OVA with $HgCl_2$.

The thermodynamics of binding can be estimated by measuring the free energy of binding ($\Delta G^0$) given by

$$\Delta G^0 = -2.0303\ RT \log K_b \qquad (2)$$

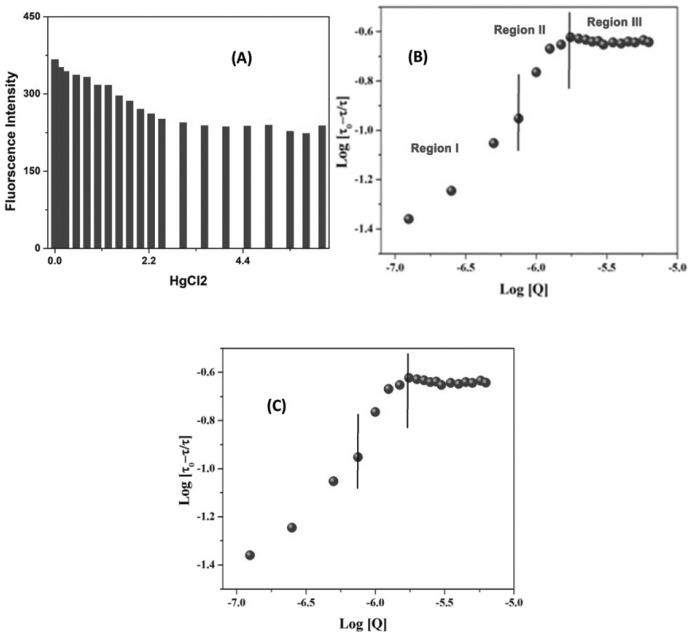


**Figure 2.** (A) Variation in the fluorescence intensity of OVA against the varying concentrations of HgCl2. (B) Plot of log [(F0-F)/F] vs log [ligand] for OVA-$HgCl_2$ at pH 2.2. The regions (I-III) represent the various binding stages of HgCl2 to OVA. (C) Plot of log $[(\tau_0-\tau)/\tau]$ against log $[HgCl_2]$ for OVA-ligand at pH 2.2.

A plot of log $[F_0-F/F]$ against log $[HgCl_2]$ is shown in figure 2B. From the figure, it is evident that the stepwise addition of $HgCl_2$ and sequential unfolding of ovalbumin involves a three state transition with the increasing concentration of $HgCl_2$. Classical linear polymerisation of protein usually has a typical sigmoid presentation. The sigmoidal curve presents a three stage process involving misfolding (lag phase), nucleation (growth phase), and fibril elongation (end phase). Lag phase is the slow process in the polymerization reaction where the 'nuclei' formation is initiated. In the second phase (growth phase) the nuclei (monomers) formed joins together to form rapidly join to form oligomers (protofibrils). This phase is thermodynamically highly favourable and is a fast process. In the saturation phase final fibril is formed (Bhak, Choe et al. 2009, Arosio, Knowles et al. 2015). To elucidate the detailed mechanism of protein aggregation the magnitudes of $K_b$, n, and ΔG binding have been estimated for the first two regions (I-II of figure 2 up to which binding of $HgCl_2$ to OVA takes place) using eqn. 1 and 2, and are summarized in table 1.

**Table 1.** Quenching constants and binding parameters of OVA-$HgCl_2$ systems at 298 K.

| pH | $Kq_1$ ($M^{-1}s^{-1}$) | $Kq_2$ ($M^{-1}s^{-1}$) | $n_1$ | $n_2$ | $K_{b1}$ ($M^{-1}$) | $K_{b2}$ ($M^{-1}$) | $\Delta G_1$ (kJ $mol^{-1}$) | $\Delta G_2$ kJ $mol^{-1}$ |
|---|---|---|---|---|---|---|---|---|
| 2.2 | $1.19\times10^{13}$ | $2.26\times10^{13}$ | 0.62 | 1.35 | 46.03 | $3.49\times10^{4}$ | -9.48 | -25.92 |

From the life time data also we obtained a three state transition state as shown in figure 2C. This further confirms the steady-state fluorescence experiments. A short lag phase was observed for the system. The molten globule state of OVA has stable secondary structural features and is devoid of tertiary structure. The thermodynamic analysis of region I of pH 2.2 shows low 'n' value indicating partial binding of $HgCl_2$ to the protein. The $K_b$ value of this region is also very low. This indicates the formation of nuclei, which is a slow process and thermodynamically unfavourable. The $\Delta G_0$ value for this region only -9.48 kJ $mol^{-1}$, indicating weaker binding. Region II shows large 'n' and $\Delta G_0$ value indicative of stronger binding. Region II demonstrates the 'growth' phase in the protein aggregation. These points out the possibility of linear polymerisation have short or lag time having all the characteristic features of nucleation dependent polymerization. There will be sequential build-up of intermediates occurs up on fibrillation pathway. The addition of 6.25 µM $HgCl_2$ (saturation phase) the width of the protofibrils intensely increased to 265 nm with no effect in the height (Fig. 3D). Increases width of the protofibrils points out the possibility of lateral addition for the fibril growth mechanisms the saturation phase.

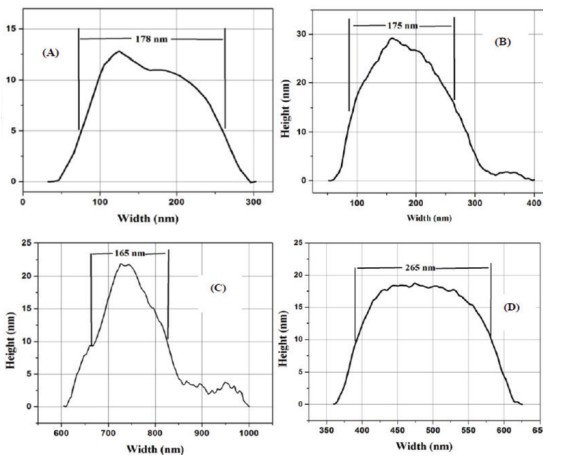


**Figure 3.** Width profile of oligomers/protofibrils (A): OVA pH 2.2 before exposure (B): after exposure to 1.25 µM $HgCl_2$; (C): with the increment of $HgCl_2$ to 2.5 µM; (D) with the increment of $HgCl_2$ to 6.25 µM

### 3.3 Time Dependent AFM Analysis

The AFM results show the formation of various oligomeric structures during the characterization. Not all protein aggregates in CNS diseases are of the amyloid fibrillar type. It is generally accepted that amyloid fibrils are just detoxification products while oligomeric intermediates are the toxic species. So in order to know whether the different protofibrils formed by the addition of $HgCl_2$ leads to fibril formation prolonged incubation of each phase (region) for 25 days were carried out and its AFM image were recorded. From the figure 4A, it is clear that with the incubation time the oligomers in the Region I joined to form long fibrils with a height of 10-30 nm (Fig. 4C) with a width of 300 nm (Fig. 4D). In region II, we can observe thicker fibrils (Fig. 4E) in which the protofibrils were combined side wise to form a thicker fiber of almost 700 nm wide (Fig. 4H). The height of the particle tremendously increased to 50- 125 nm (Fig. 4G). During the region III, thicker and longer fibers (Fig. 4I) were formed with ~ 1 µm (Fig. 4L) width suggesting that the protofibrils are self-assembled laterally during the prolonged incubation. The height is found to be in between 25-200 nm (Fig. 4K). Such micrometer-sized thicker fibrils obtained for peptide mixtures were reported by Justin R. Barone et al.

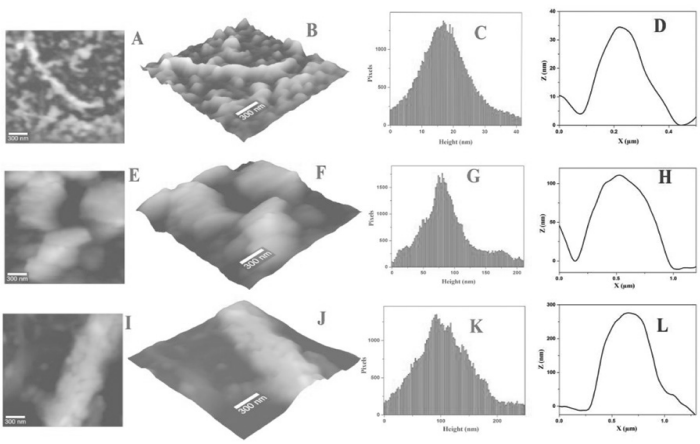


**Figure 4:** (A):Long fibrils and protofibril formation of OVA with the addition of 1.375 µM HgCl2 after the incubation of 25 days (B): (C): and (D): the corresponding 3D representation, height and width profile; (E): Thick micrometer sized fibril formation of OVA with the addition of 2.5 µM HgCl2 after the incubation of 25 days; (F): (G): and (H): the corresponding 3D representation, height and width profile; Thick long straight fibril formation of OVA with the addition of 6.25 µM HgCl2 after the incubation of 25 days; (F): (G): and (H): the corresponding 3D representation, height and width profile.

## 4. Conclusion

Herein, we report the mechanism of formation of defolded state of ovalbumin, a model serpin at acidic pH on exposure to increasing concentration of mercuric chloride. We combine different spectroscopic and microscopic techniques to study the possible share of environmental toxins in inducing protein misfolding and hence protein aggregation. The fluorescence interaction study of mercuric chloride, a heavy metal toxin, with OVA brings about more insight, without doubt, into the mechanistic aspects; but to a large extent the perturbation it can cause to the protein conformation. Critical role of the oligomeric species isolated in the middle of fibrillation process should be acknowledged to evaluate the mechanism of amyloid fibril formation by acting as the seeds or the growing unit for the fibrillar assembly, in addition to their suggested pathological activity of causing cytotoxicity.

## Reference


Albrecht, C. (2008). "Joseph R. Lakowicz: Principles of fluorescence spectroscopy, 3rd Edition." Analytical and Bioanalytical Chemistry **390**(5): 1223-1224.

Anand, U., C. Jash and S. Mukherjee (2010). "Spectroscopic Probing of the Microenvironment in a Protein−Surfactant Assembly." The Journal of Physical Chemistry B **114**(48): 15839-15845.

Arosio, P., T. P. Knowles and S. Linse (2015). "On the lag phase in amyloid fibril formation." Phys Chem Chem Phys **17**(12): 7606-7618.

Bhak, G., Y. J. Choe and S. R. Paik (2009). "Mechanism of amyloidogenesis: nucleation-dependent fibrillation versus double-concerted fibrillation." BMB Rep **42**(9): 541-551.

Bhattacharya, M. and P. Dogra (2015). "Self-Assembly of Ovalbumin Amyloid Pores: Effects on Membrane Permeabilization, Dipole Potential, and Bilayer Fluidity." Langmuir **31**(32): 8911-8922.

Bhattacharya, M. and S. Mukhopadhyay (2012). "Structural and Dynamical Insights into the Molten-Globule Form of Ovalbumin." The Journal of Physical Chemistry B **116**(1): 520-531.

Dalal, V., S. Arya, M. Bhattacharya and S. Mukhopadhyay (2015). "Conformational Switching and Nanoscale Assembly of Human Prion Protein into Polymorphic Amyloids via Structurally Labile Oligomers." Biochemistry **54**(51): 7505-7513.

Gettins, P. G. W. (2002). "Serpin Structure, Mechanism, and Function." Chemical Reviews **102**(12): 4751-4804.

Hatcher, L. Q., L. Hong, W. D. Bush, T. Carducci and J. D. Simon (2008). "Quantification of

the Binding Constant of Copper(II) to the Amyloid-Beta Peptide." The Journal of Physical Chemistry B **112**(27): 8160-8164.

Ibrahim, N., H. Ibrahim, S. Kim, J.-P. Nallet and F. Nepveu (2010). "Interactions between Antimalarial Indolone-N-oxide Derivatives and Human Serum Albumin." Biomacromolecules **11**(12): 3341-3351.

Jacobsen, J. S., P. Reinhart and M. N. Pangalos (2005). "Current concepts in therapeutic strategies targeting cognitive decline and disease modification in Alzheimer's disease." NeuroRx **2**(4): 612-626.

Lamba, J., S. Paul, V. Hasija, R. Aggarwal and T. K. Chaudhuri (2009). "Monitoring protein folding and unfolding pathways through surface hydrophobicity changes using fluorescence and circular dichroism spectroscopy." Biochemistry (Moscow) **74**(4): 393-398.

Lopes de Andrade, V., A. P. Marreilha Dos Santos and M. Aschner (2021). "NEUROTOXICITY OF METAL MIXTURES." Adv Neurotoxicol **5**: 329-364.

Mathew, M., S. Sreedhanya, P. Manoj, C. T. Aravindakumar and U. K. Aravind (2014). "Exploring the Interaction of Bisphenol-S with Serum Albumins: A Better or Worse Alternative for Bisphenol A?" The Journal of Physical Chemistry B **118**(14): 3832-3843.

Pan, Y., B. Wang, T. Zhang, Y. Zhang, H. Wang and B. Xu (2016). "Nanoscale insights into full-length prion protein aggregation on model lipid membranes." Chemical Communications **52**(55): 8533-8536.

Squitti, R. and R. Polimanti (2013). "Copper phenotype in Alzheimer's disease: dissecting the pathway." American journal of neurodegenerative disease **2**(2): 46-56.

Tamás, M. J., B. Fauvet, P. Christen and P. Goloubinoff (2018). "Misfolding and aggregation of nascent proteins: a novel mode of toxic cadmium action in vivo." Curr Genet **64**(1): 177-181.

Tamás, M. J., S. K. Sharma, S. Ibstedt, T. Jacobson and P. Christen (2014). "Heavy metals and metalloids as a cause for protein misfolding and aggregation." Biomolecules **4**(1): 252-267.